



# Mechanical Properties of Laser Shock-Peened Regions of SS316LN and SS304 Studied by Nanoindentation

Pardhu Yella<sup>1</sup> · J. Varghese<sup>1</sup> · P. Prem Kiran<sup>2</sup> · R. K. Buddu<sup>3</sup> · K. Bhanu Sankara Rao<sup>4</sup> · Koteswararao V. Rajulapati<sup>1</sup>

Received: 7 May 2019 / Accepted: 16 October 2019 / Published online: 1 November 2019  
© Indian National Academy of Engineering 2019

## Abstract

Nanoindentation has been used to evaluate various mechanical properties of affected regions of laser shock-peened (LSP) stainless steels, SS316LN and SS304 plates. Depending on the applied laser parameters (laser energy, pulse width), the hardness was varied in the range 3.5–6.2 GPa in comparison with the untreated sample hardness of 2.93 GPa for SS316LN. Similarly in SS304, the hardness has been improved to 5.73 GPa in comparison with the untreated specimen hardness of 2.57 GPa. The improvement in the hardness for the laser-treated stainless steel targets is attributed to various factors viz., increment in internal frictional stress, dislocation–dislocation interaction and solute–dislocation interactions. Effect of laser energy is not appeared in the hardness values but a difference in hardness values with the pulse width has been observed. The deformation characteristics such as strain rate sensitivity and activation volume were evaluated from the indentation creep data. Notable change in the strain rate sensitivity is not observed for the laser-treated samples in comparison with the untreated samples and the range of values measured between 0.01 and 0.02. The activation volumes for both the treated and untreated samples were in the range, 100–200 b<sup>3</sup>. There was a slight decrease in activation volume in the laser-treated samples. Several rate-controlling deformation mechanisms appear to be operative in these treated samples, in addition to the dislocation-based mechanisms.

**Keywords** Laser shock peening · Nanoindentation · Stainless steel · Strain rate sensitivity · Activation volume

## Introduction

Stainless steels SS316LN and SS304 are used as strategic structural materials in the nuclear industry because of their potential advantages (Suri et al. 2010). These structural materials possess many attractive mechanical properties, such as high strength, ductility, desirable toughness, high work hardening ability, and excellent corrosion resistance (Mannan et al. 2003). However, these steels retain moderate

fatigue strengths and the surface treatment techniques like shot peening (Sara Bagherifard 2012), laser shock peening (Kalainathan and Prabhakaran 2016) and ultrasonic treatment (Mordyuk et al. 2008) techniques are performed on these steels for better fatigue lives. Among all the other surface treatment techniques, laser shock peening (LSP) is preferred because of its precise control over the residual stresses, surface roughness and hardness on the surface (Montross et al. 2002).

The thin layer of laser-hardened stainless steel surface and its damage associated with the shock peening pose significant challenges in quantification of mechanical properties of the “thin peened region”. The best common method to analyze the effect of surface hardening and the mechanical properties of alloys/steels is through nanoindentation (Saleh et al. 2016). Compared to other methods such as micro/nano-pillar compression (Grieverson et al. 2012; Sharon et al. 2013), cantilever bending (Armstrong et al. 2015) and tensile testing (Reichardt et al. 2015), nanoindentation is the easy method to examine the effect of input laser parameters on the hardened stainless steel surfaces (Hardie et al. 2015;

✉ Koteswararao V. Rajulapati  
kvrse@uohyd.ernet.in

<sup>1</sup> School of Engineering Sciences and Technology, University of Hyderabad, Hyderabad 500046, India

<sup>2</sup> Advanced Centre of Research in High Energy Materials (ACRHEM), University of Hyderabad, Hyderabad 500046, India

<sup>3</sup> FRMDC Division, Institute for Plasma Research, Bhat, Gandhinagar 382428, India

<sup>4</sup> Pratt and Whitney Chair, University of Hyderabad, Hyderabad 500046, India

Hattar et al. 2012). There are several advantages in performing the nanoindentation on the laser-treated surfaces such as ease of experiment, relative simplicity in sample preparation and comfort of applying the indents on the top laser-treated surface allows to explore the mechanical properties and deformation characteristics. Many research investigations by different authors (Dayal et al. 2013; Hosemann et al. 2008, 2009, 2012) have resulted in exploration of various mechanical properties on wide variety of materials using nanoindentation.

Using nanoindentation, the hardness has been assessed for the surface-treated stainless steels by various methods such as ion irradiation, LSP, ultrasonic treatments. Ma et al. (Ma and Ling 2011) improved the hardness up to 38% for the stainless steel SS304 using ultrasonic impact treatment with a surface hardened layer of 450–500  $\mu\text{m}$ . Montross et al. (2001) studied the self-limiting hardness by Hugoniot Elastic limit (HEL) in laser-peened 6061-T6 aluminum. For the higher shock wave pressure (6 GPa)-treated aluminum samples, hardness was increased when compared to lower shock wave pressure (3.5 GPa) for both one and five repetitions. However, in all these studies for the alloys explored, the cause of improving the hardness has not been forecasted.

Even though a lot of studies have been dedicated to evaluate the hardness of the surface-treated stainless steels, much data are lacking in evaluating the strain rate sensitivity (SRS) and activation volume. Thus, in the present article systematically, the variation in hardness with respect to the input laser parameters viz., laser energy and laser pulse duration has been extracted using nanoindentation data. Further from the indentation creep, the strain rate sensitivity and the activation volumes are calculated to assess the rate-controlling deformation mechanisms in the hardened surface of stainless steels.

## Experimental details

Austenitic stainless steels used in this study, SS316LN and SS304 have been supplied by M/s Mishra Dhatu Nigam Ltd (MIDHANI), Hyderabad, India with the chemical composition as given in Table 1.

From the as-received material which were hot rolled and annealed at 1100  $^{\circ}\text{C}$ , plates of dimensions 12 mm  $\times$  12 mm  $\times$  6 mm were extracted through electric discharge machining (EDM). Further, the sample surfaces were polished through different graded emery papers to

attain a surface roughness of 0.1  $\mu\text{m}$ . Using second harmonic of Nd: YAG laser (532 nm, 10 Hz), the polished surface was subjected to laser shock peening. Two pulse widths (viz., 30 ps and 7 ns) are used in the current study. The laser energy was varied from 5 mJ to 25 mJ with steps of 5 mJ for 30 ps and 30 mJ to 90 mJ with steps of 30 mJ for 7 ns, respectively. Various sacrificial layers have been adapted including an absorbent adhesive tape to confine the plasma and these details were presented comprehensively in refs. (Yella et al. 2018a, b, 2019). The residual stresses reported were measured using the X-ray diffraction technique with  $\sin^2\psi$  method. As the usage of absorbent adhesive tape has resulted in significant compressive residual stresses in both SS316LN and SS304 with less surface damage (Figs. 1 and 2), nanoindentation was performed on the samples covered with absorbent adhesive tape during peening. The surface roughness, residual stress and dislocation density data pertaining to various peened samples are presented in Table 2.

Hysitron's TI950 Triboindenter with a Berkovich diamond indenter has been used. The load was increased at different rates (80, 160, 450, 800, 2500, 5000 and 7000  $\mu\text{N/s}$ ) at the peak load of 8000  $\mu\text{N}$ . The load was held at the peak value for 10 s before unloading. The load–time history followed is shown in Fig. 3. Loading rates for each peak force are selected in such a way that the strain rate changes by an order or half the order of magnitude to attain each datum point. Each test was repeated 25 times under identical test conditions by performing a  $5 \times 5$  matrix for achieving better accuracy in the results, and the spacing between two consecutive indents was maintained at 3  $\mu\text{m}$  (Fig. 4). Strain rate sensitivity (SRS) was calculated for a single indent, following the method described in ref. (Alkorta et al. 2008). Thus, obtained SRS values were considered and average of them is reported as a SRS value for the given condition; error bars represent the standard deviation in these values obtained for a given test condition.

## Results and discussion

In case of SS316LN treated at a laser pulse width of 30 ps, as the laser energy has increased, compressive stresses have also increased to a value of  $-695$  MPa at 25 mJ (Table 2). When the same sample was peened at a pulse width of 7 ns, the compressive stress was about  $-805$  MPa (at 90 mJ). The surface roughness has also increased to a value of 0.124 (for ps treated)  $\mu\text{m}$  at 25 mJ of energy and to 0.665  $\mu\text{m}$  (for

**Table 1** Chemical composition of SS316LN and SS304 (in wt%) used in the present study

S. No.	Materials used	C	Mn	Ni	Cr	Mo	N	S (max)	P (max)	Fe
1	SS316LN	0.025	1.75	12.0	17.0	2.4	0.11	0.002	0.023	Balance
2	SS304	0.055	1.50	12.0	17.5	2.3	–	0.01	0.025	Balance

**Fig. 1** Surface profiles of laser-treated stainless steel SS316LN with absorbent adhesive tape for laser peening conditions of **a** 30 ps, 15 mJ **b** 30 ps, 25 mJ **c** 7 ns, 30 mJ and **d** 7 ns, 90 mJ

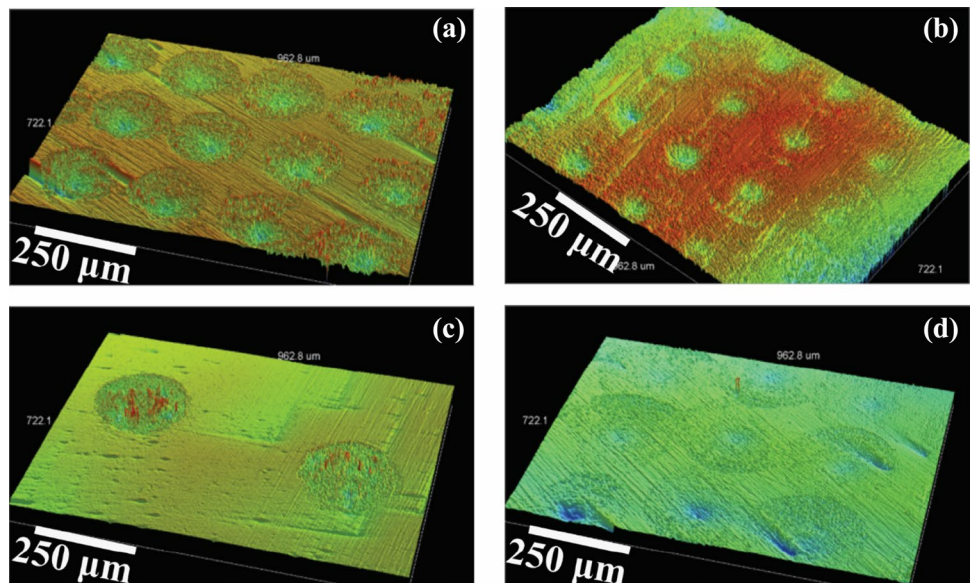
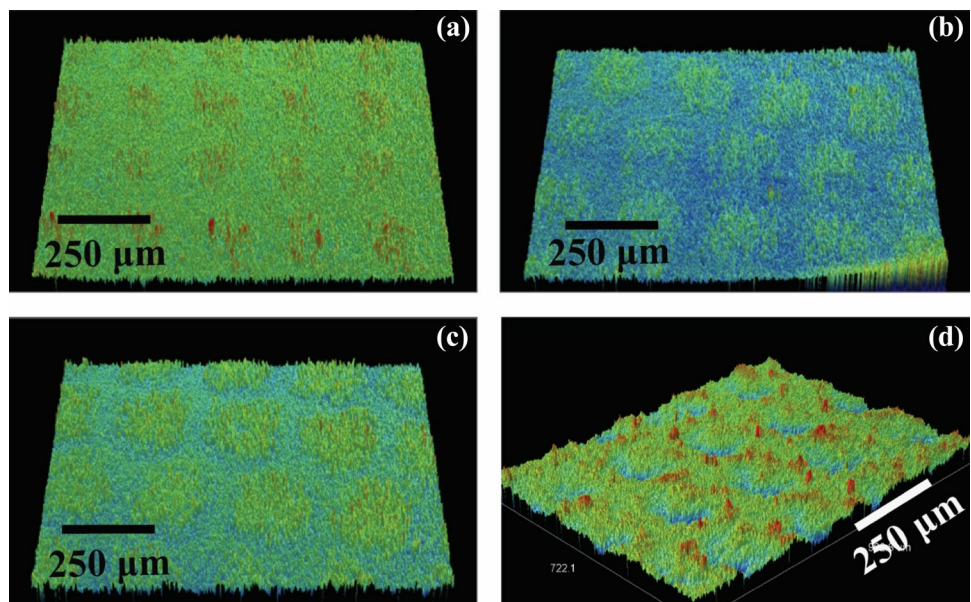


**Fig. 2** Surface profiles of laser-treated stainless steel SS304 with absorbent adhesive tape for laser peening conditions of **a** 30 ps, 15 mJ **b** 30 ps, 25 mJ **c** 7 ns, 30 mJ and **d** 7 ns, 90-mJ samples



ns treated) in comparison to 0.046 μm for untreated sample. The dislocation density in the untreated sample was  $81 \times 10^{13} \text{ m}^{-2}$  in the laser-treated sample and it has increased to  $635 \times 10^{13} \text{ m}^{-2}$  (for 30 ps and 25 mJ) and  $289 \times 10^{13} \text{ m}^{-2}$  (for 7 ns and 90 mJ).

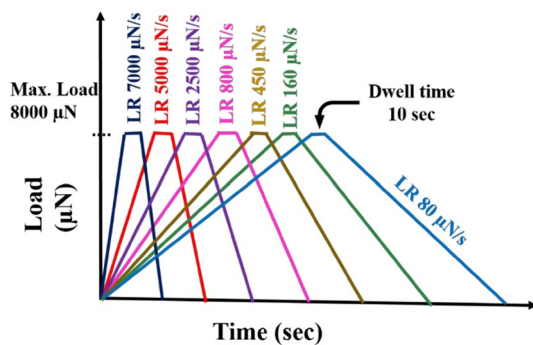
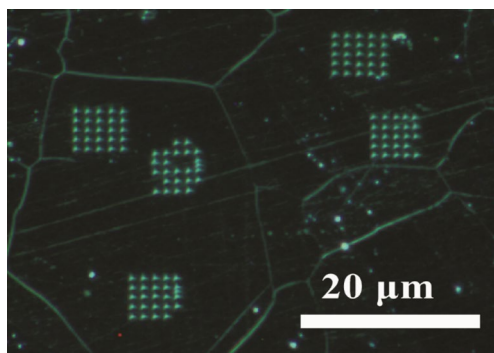
In line with the trends observed for SS316LN, the surface roughness, residual stress and dislocation densities have also increased as the laser energy is increased at both the pulse widths employed. Table 2 comprehensively presents these data.

The samples covered with absorbent adhesive tape have resulted in high compressive residual stresses and high dislocation densities with less surface damage. Therefore, the surface mechanical properties of these samples (SS316LN

and SS304) were studied by nanoindentation (Fig. 2) at room temperature and reported here. Typical load displacement curves obtained for untreated, laser-treated samples are shown in Fig. 5 and it is evident that the indentation response is uniform for a given test condition and a given sample. The hardness was deduced from unloading part of the curve following the Oliver–Pharr method (Oliver and Pharr 1992, 2004). These hardness data obtained at various loading rates employed during nanoindentation are presented in Fig. 6. It is clear that as the laser energy has increased, there was a significant improvement in the hardness of these samples in comparison to the hardness of the untreated sample. This increment in hardness would be arising from high amount of residual stresses, increased dislocation densities, etc.

**Table 2** Variation in surface roughness, residual stress and dislocation densities of untreated and different laser-treated stainless steel samples

Material	Pulse duration (s)	Laser energy (mJ)	Surface roughness ( $\mu\text{m}$ )	Residual Stresses (MPa)	Dislocation density ( $\times 10^{13}$ ) ( $\text{m}^{-2}$ )	
SS316LN	30 ps	Untreated	0.046	– 73	81	
		5	0.047	– 548	249	
		10	0.049	–	371	
		15	0.081	– 589	419	
		20	0.096	–	586	
		25	0.124	– 695	635	
	7 ns	30	0.0517	– 116	277	
		60	0.0556	– 461	283	
		90	0.06656	– 805	289	
SS304	30 ps	Untreated	0.046	– 65	28	
		10	0.085	–	390	
		15	0.114	– 492	416	
		20	0.105	–	387	
		25	0.088	– 663	461	
		30	0.08586	– 262	201	
	7 ns	60	0.12	– 272	242	
		90	0.566	– 356	266	

**Fig. 3** Load vs. time history followed to obtain the surface deformation characteristics**Fig. 4** The indented region of the untreated specimen

To critically analyze the hardness data, the averaged data are presented in Table 3. For SS316LN sample, the untreated condition had a hardness of 2.93 GPa and it increased to as high as 5.14 GPa and 4.05 GPa for 30 ps and 7 ns conditions, respectively. It amounts to increments of 175% and 138%, respectively. For SS304 sample, the untreated condition possessed a hardness value of 2.57 GPa and it increased to as high as 5.73 GPa and 3.56 GPa for 30 ps and 7 ns conditions, respectively. This increment in hardness corresponds to 223% and 138%, respectively.

It is well established that the strength of a polycrystalline solid gets influenced by various parameters such as applied load, loading rate, temperature and microstructure. To understand the influence of loading rate on the overall mechanical behavior of the peened region of both the samples, nanoindentation was performed by varying loading rate at a constant peak load and room temperature. It is assumed that microstructure of the sample is uniform throughout the peened region and it does not change dynamically during testing. The load displacement characteristics of the hold region (10 s) during nanoindentation are shown in Fig. 7 and these are fitted with the Eq. (1), following the procedure presented in the ref. (Chinh and Szommer 2014; Alkorta et al. 2008; Sudharshan Phani et al. 2017).

$$h = B(t - t_c)^{(m/2)}, \quad (1)$$

where  $h$  is indentation depth,  $B$  and  $t_c$  are constants;  $t$  is the time. “ $m$ ” gives the value of strain rate sensitivity. All

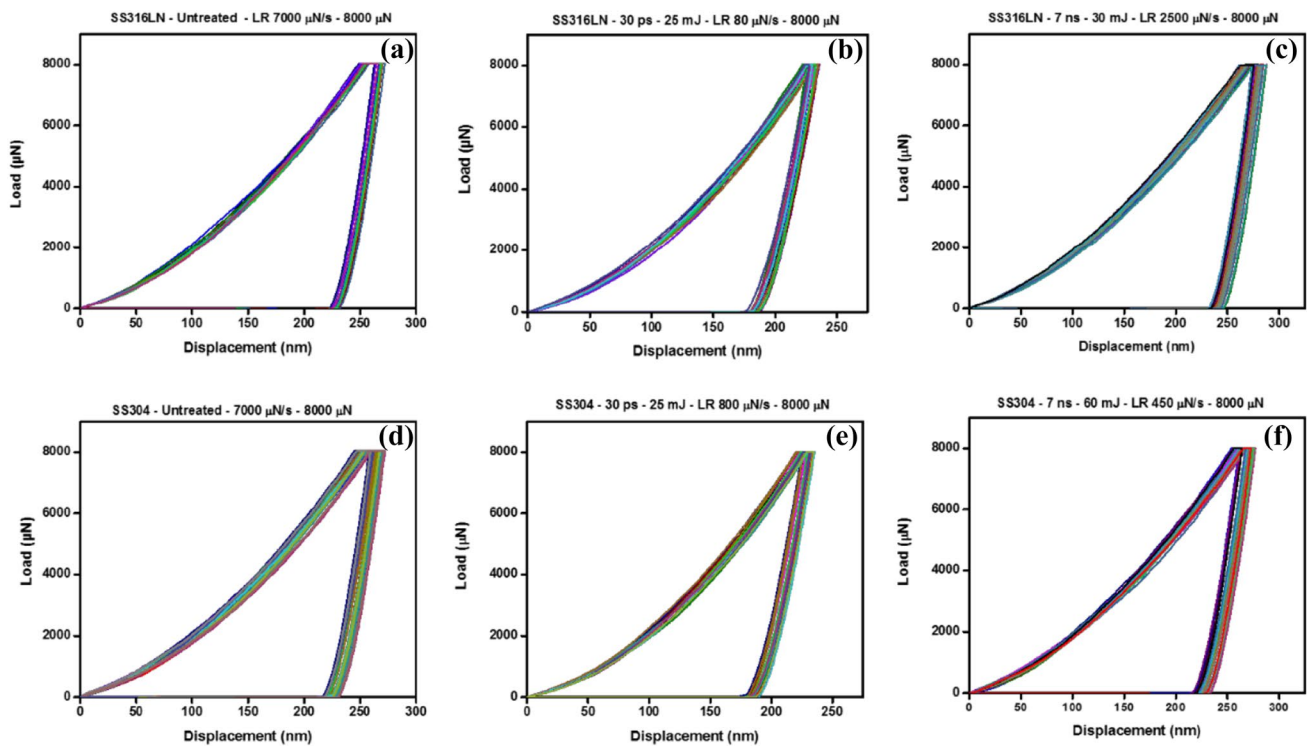


**Fig. 5** Load–displacement curves obtained at a peak load of 8000 µN for **a** SS316LN, untreated **b** SS316LN, 30 ps **c** SS316LN, 7 ns **d** SS304, untreated **e** SS304, 30 ps **f** SS304, 7-ns samples

the curves are fitted to the above equation with an adjusted  $R^2$  value better than 0.99 (Fig. 7). The indentation depth and time were normalized with their corresponding highest values obtained during testing. These normalized plots can be seen in Fig. 8 and it is evident that indentation response does change with the loading rate in the given hold time for various samples. It is also clear that as the loading rate is increased, at a given time the indentation depth decreases indicating towards increased hardness values. The increment in hardness with increase in loading rate for a given test condition and a given sample suggests that the loading rate response is positive leading to positive strain rate sensitivity. Thus, obtained SRS values are presented in Fig. 9. It is clear that irrespective of the sample nature (SS316LN or SS304) and peened conditions (30 ps or 7 ns), the SRS has assumed values between 0.01 and 0.02. It is also striking to observe that the SRS value of peened samples is slightly less than that for untreated sample.

The activation volume ( $V^*$ ) is calculated from the strain rate sensitivity values (Fig. 10) and the corresponding hardness values (Table 3) using the Eq. (2).

$$V^* = 3\sqrt{3}k_B T \frac{\partial \ln(\dot{\epsilon})}{\partial \ln H}, \quad (2)$$

where  $k_B$  is the Boltzmann constant,  $T$  is the absolute temperature (300 K),  $H$  is the hardness and  $m$  is the strain rate

sensitivity. The obtained activation values ( $100\text{--}200\text{ b}^3$ ,  $b$  is the Burgers vector of the given material) are shown in Fig. 10. It is evident that the activation volumes are decreasing with the applied laser energy for all the laser peening conditions. For both the SS304 and SS316LN the activation volumes are decreasing suggesting the involvement of different rate-controlling mechanisms in comparison to those for untreated sample.

As it can be seen in Figs. 1 and 2, the surface damage was minimal for both SS316LN and SS304 plates during LSP when they were covered with adhesive absorbent tape. The damage on the surface was minimal when adhesive absorbent tape was used as a sacrificial layer and the surface damage was more when no sacrificial layer was used. Detailed microstructural details are given in (Yella et al. 2018a, b). Table 2 presents some of the key characteristics such as surface roughness, residual stress and dislocation density. It is clear that the surface roughness values are insignificant. All the residual stresses are compressive in nature and the dislocation density has increased with increase in laser energy. As the energy has increased during LSP, atomic level displacements might have resulted in the increased dislocation densities which in turn would have resulted in increased lattice microstrain (Yella et al. 2018a, b). It is clear that the LSP has resulted in significant improvement in the hardness of the peened region. The increase in hardness as shown in

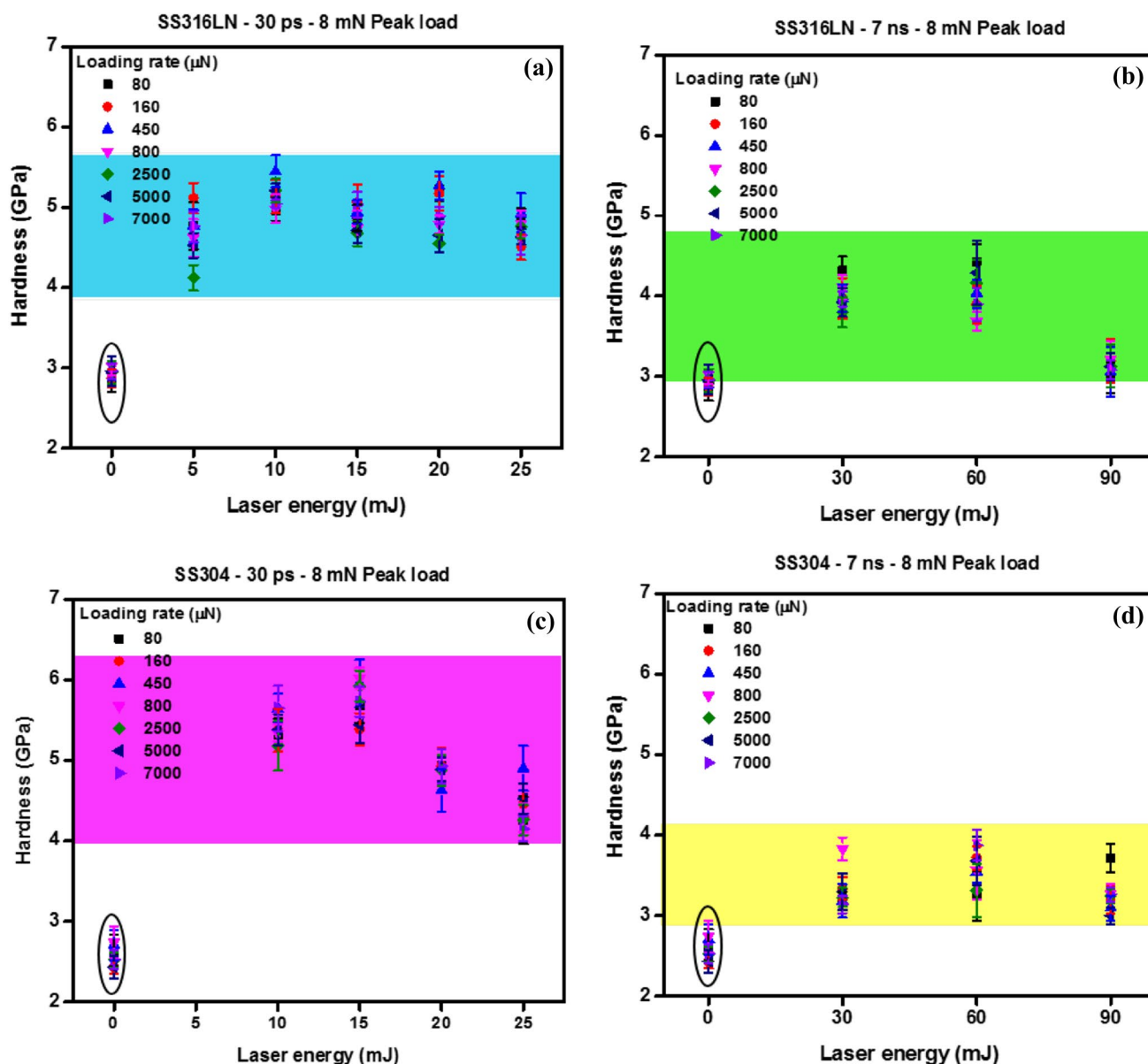


**Fig. 6** Variation of hardness with different laser energies applied for **a** SS316LN, 30 ps **b** SS316LN, 7 ns **c** SS304, 30 ps and **d** SS304, 7-ns samples. The data at laser energy of “0” represent untreated sample

Fig. 6 could be having the origins from one or more of the following:

- increased lattice frictional stress
- dislocation–dislocation interactions
- dislocation–solute interactions

It is interesting to observe that the SRS did not show much change between untreated and treated samples. However, there was slight decrease in the activation volume to  $100 \text{ b}^3$  from about nearly  $200 \text{ b}^3$ . In conventional polycrystalline materials, dislocation-based mechanisms would result

in an activation volume close to  $1000 \text{ b}^3$ . In nanocrystalline multi-phase, an activation volume of close to  $10 \text{ b}^3$  was observed (Varam et al. 2014a, b, 2016). However, in the current materials which were subjected to LSP, we have observed a reduction in it by an order of magnitude. This suggests that other lattice defects such as vacancies, stacking faults, twins, etc. which could have formed during LSP might also be playing a key role in deciding the activation volume in these materials.

Sharma et al. (2011) investigated the effect of 4.0 MeV proton irradiation on the microstructure and mechanical properties of nanocrystalline (nc) nickel foils on SS

**Table 3** Variation of hardness with applied laser parameters (averaged for all loading rates at a given condition)

Material	Pulse duration (s)	Laser energy (mJ)	Hardness (GPa)	
SS316LN	30 ps	Untreated	2.93 ± 0.07	
		5	4.66 ± 0.30	
		10	5.14 ± 0.17	
		15	4.86 ± 0.16	
		20	4.94 ± 0.29	
		25	4.74 ± 0.14	
		7 ns	30	4.01 ± 0.16
			60	4.05 ± 0.25
			90	3.11 ± 0.07
SS304	30 ps	Untreated	2.57 ± 0.12	
		10	5.41 ± 0.17	
		15	5.73 ± 0.25	
		20	4.86 ± 0.10	
		25	4.40 ± 0.25	
		7 ns	30	3.31 ± 0.23
			60	3.56 ± 0.22
			90	3.25 ± 0.22

substrate. With an increase in hardness, the activation volume decreased more rapidly for unirradiated nc-Ni as compared to irradiated Ni. In unirradiated nc-Ni, the rate-controlling deformation mechanism is associated with dislocation density increment with the increase in stress during the course of indentation/deformation. In irradiated specimens, the deformation is associated with dislocation generation and radiation-induced defects (vacancy–interstitial clusters, dislocation–dislocation loops). In the present study, the activation volume of the laser-irradiated stainless steels has decreased slightly up to  $200 b^3$  suggesting that the rate-controlling deformation is associated with the dislocation generation and radiation-induced defects.

Kasada et al. 2016 examined strain rate sensitivity (SRS) before and after 10.5 MeV Fe<sup>3+</sup> ion irradiation up to 10 dpa at 300 °C on a single crystal Fe–15Cr–20Ni austenitic steel using a strain rate jump (SRJ) nanoindentation test. With the ion irradiation, the hardness values were increased (from 2 GPa to 3.5 GPa) at the narrow depth region but the SRS values (0.02 to 0.01) are decreased slightly. Similarly, in our study for the laser-treated samples, SRS values were decreased slightly for the laser-treated samples in comparison with the untreated sample.

Maier-Kiener and Durst 2017) studied the quantitative changes viz., different material modifications, loading rates,

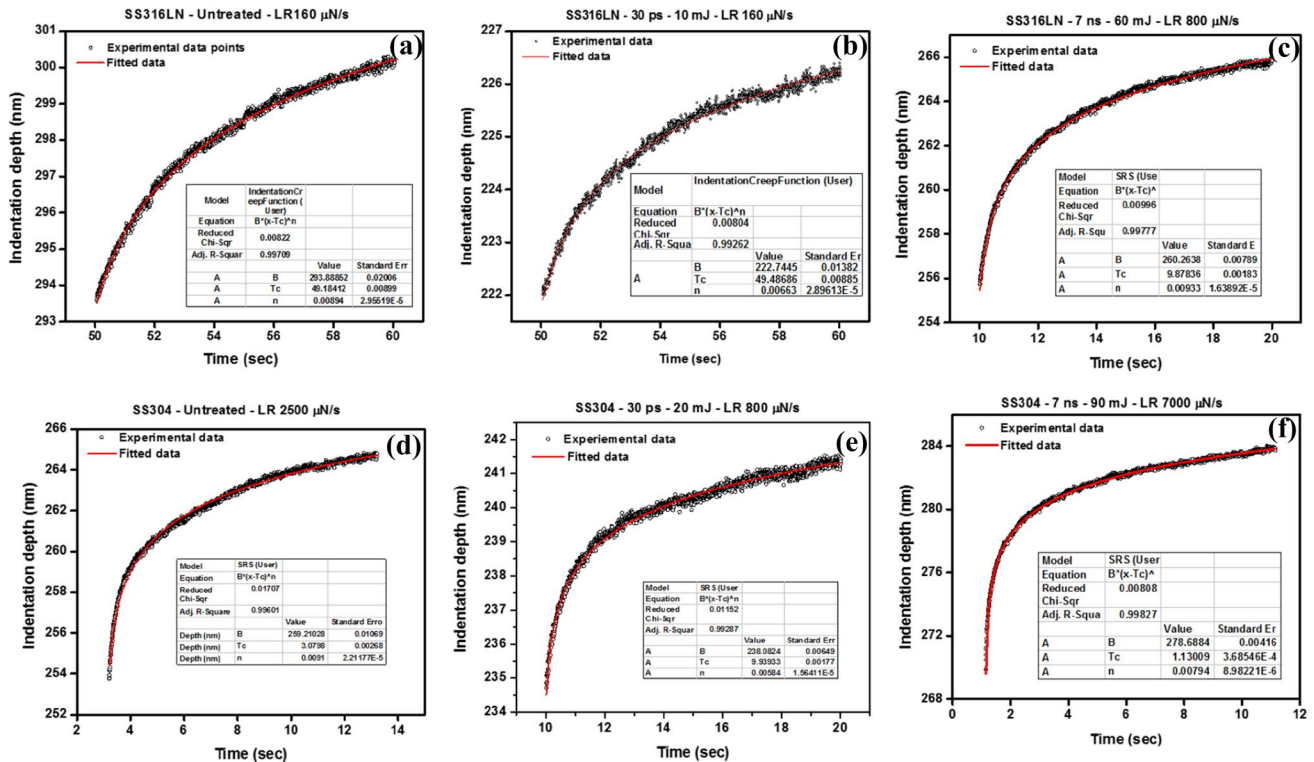


**Fig. 7** Indentation depth vs. time plots (corresponding to only hold regions of the data presented in Fig. 3) used to obtain strain rate sensitivity of **a** SS316LN, untreated **b** SS316LN, 30 ps **c** SS316LN, 7 ns **d** SS304, untreated **e** SS304, 30 ps **f** SS304, 7-ns samples

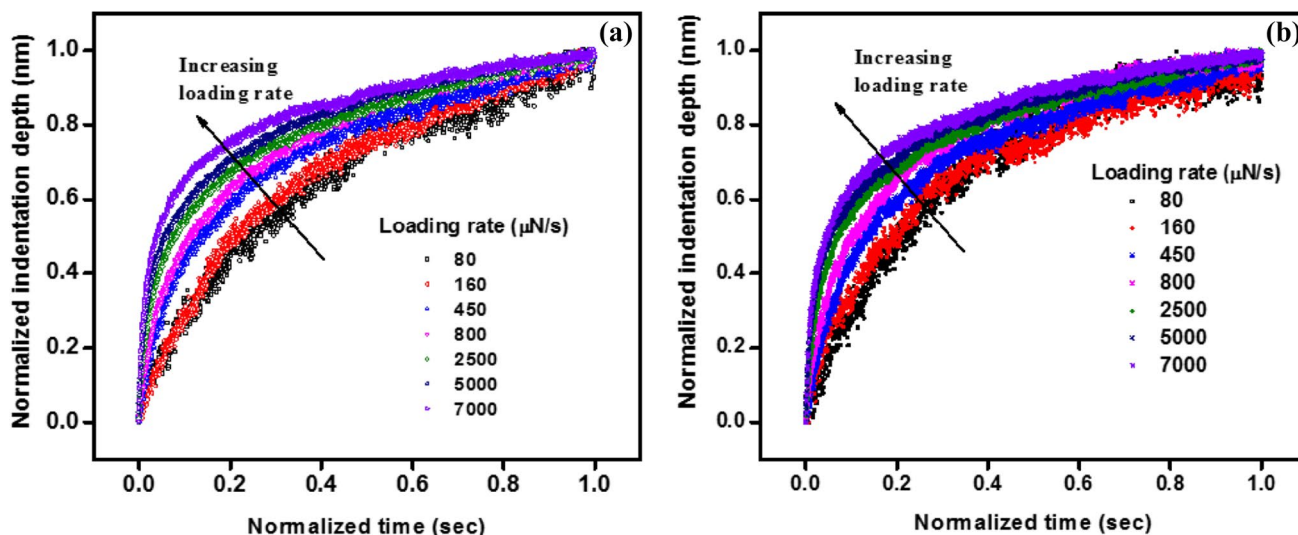


**Fig. 8** Normalized indentation depth vs. normalized time for different loading rates corresponding to “hold (constant load)” region of the **a** untreated SS304 sample and **b** laser-treated SS316LN, 30 ps, 5 mJ

sample. The effect of loading rate on indentation response at constant load is clearly evident

or temperatures are indicative of the interaction, competition, and change of different contributing plasticity mechanisms. For coarse-grained FCC materials, the primary thermal activation obstacles at low and intermediate strain rates are forest dislocations. In their study, it is concluded that the crystal structure, microstructure, and testing temperature significantly influence the deformation behavior.

The range of hardness values observed for the 30-ps laser-treated samples is higher than that of the 7-ns treated samples. These higher hardness values for the 30 ps are might be due to conceal of laser interaction with the laser-produced plasma, i.e., the plasma does not absorb any laser energy. Therefore, the entire energy of the laser is deposited on the target materials SS304 and SS316LN resulted in the increment in the hardness values. Nakano et al. (2010) also observed the increase in hardness values for the femto-second laser-treated samples in comparison to nano-second laser-treated stainless steels SS304. In comparison to all these studies, the hardness increment has been very significant in the present studies. In addition, SRS, activation volume data as well as discussion on probable rate-controlling mechanisms brings uniqueness to these studies.

## Conclusions

Mechanical properties such as hardness, strain rate sensitivity and activation volume are evaluated using nanoindentation for the laser shock-peened stainless steels SS316LN and SS304 at room temperature. With the LSP, the hardness is increased to 6.2 GPa, in comparison with the untreated sample hardness of 2.93 GPa for SS316LN. Similarly, the hardness has been improved up to 5.73 GPa in comparison with the untreated specimen (2.57 GPa) for SS304 sample. Various factors such as increment in lattice frictional stress, dislocation–dislocation interaction and solute–dislocation interactions might have led to the improvement in the hardness for the laser-treated stainless targets. The effect of laser energy within the laser pulse width has not affected the hardness values. But the effect of pulse width on hardness values is substantial. Strain rate sensitivity and activation volume were evaluated from the indentation creep data and prominent change in the strain rate sensitivity (0.01 to 0.02) is not observed between treated and untreated regions. The reduction in activation volume to  $\sim 100 \text{ b}^3$  for the laser-treated regions from  $\sim 200 \text{ b}^3$  in the untreated regions indicates the presence of several rate-controlling deformation mechanisms in addition to dislocation-based mechanisms in the peened regions.



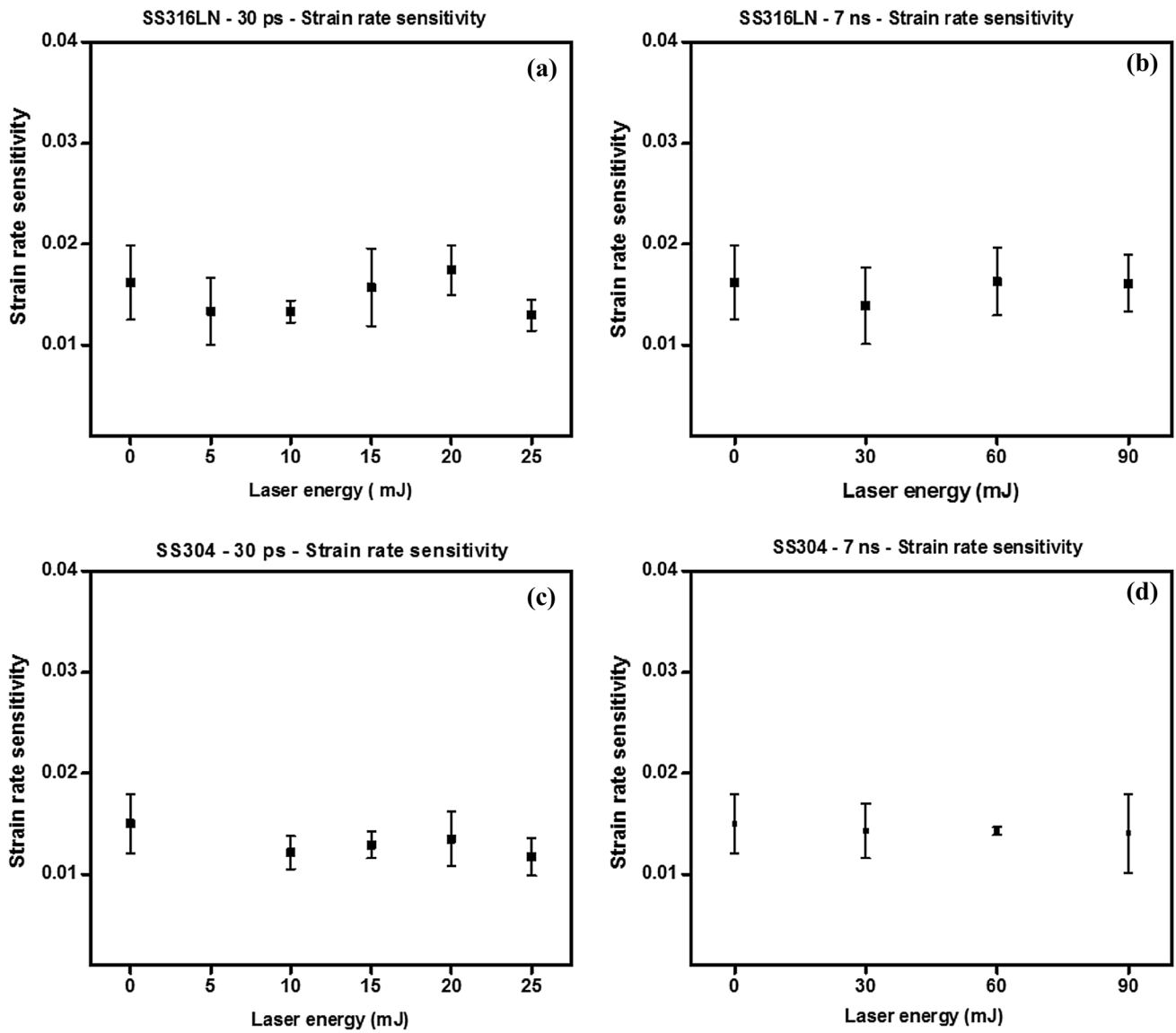


**Fig. 9** Variation of SRS values obtained at constant load, for various applied laser parameters **a** SS316LN, 30 ps **b** SS316LN, 7 ns **c** SS304, 30 ps and **d** SS304, 7-ns samples. The data at laser energy of “0” represent untreated sample

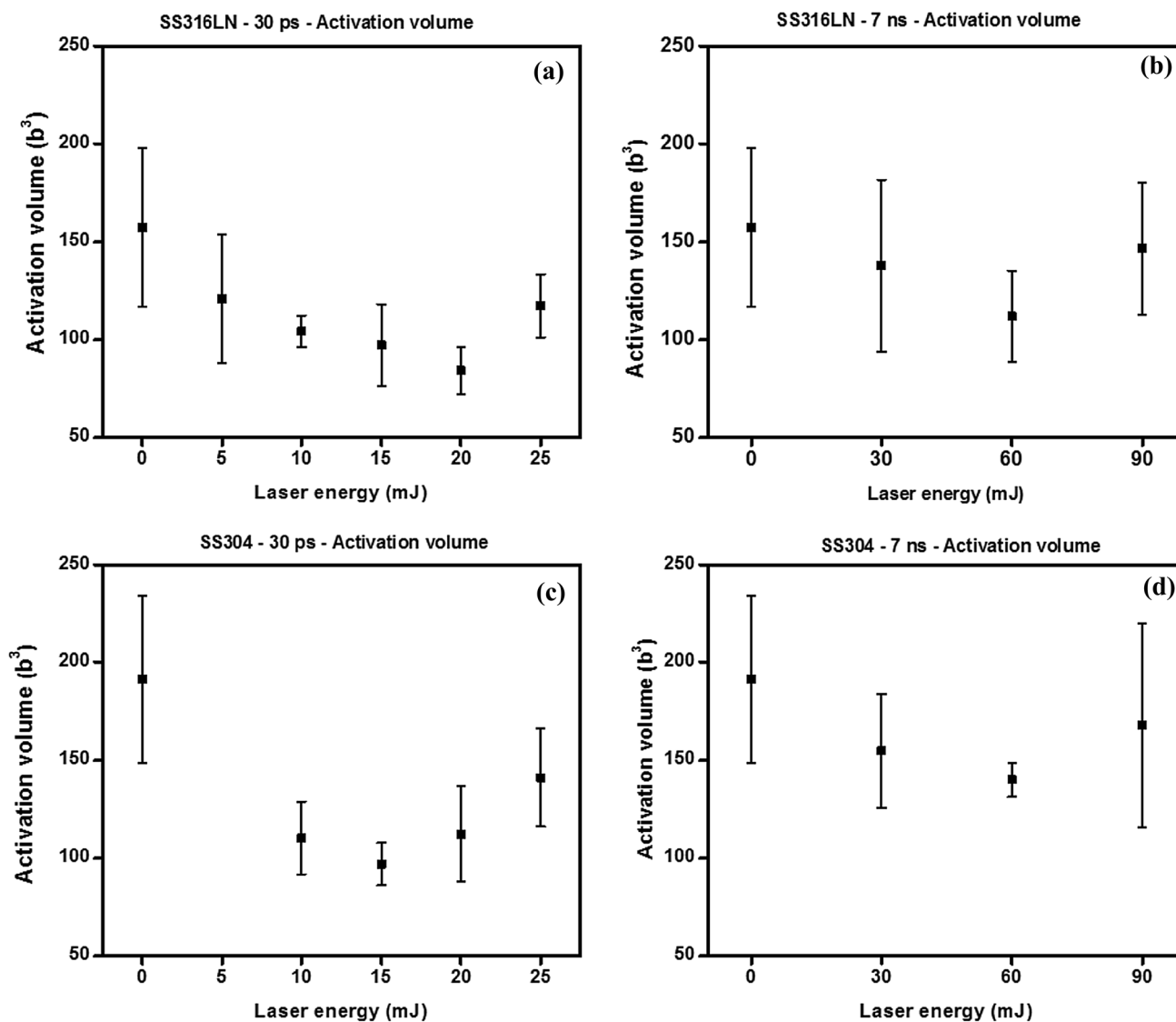


**Fig. 10** Variation of activation volume with applied laser parameters for **a** SS316LN, 30 ps **b** SS316LN, 7 ns **c** SS304, 30 ps **d** SS304, 7-ns samples. The data at laser energy of “0” represent untreated sample

**Acknowledgements** This research work is supported by the Board of Research in Fusion Science and Technology (BRFST) under grant, NFP/MAT/A12-04, Department of Atomic Energy, Government of India. The authors gratefully acknowledge DST-PURSE program of University of Hyderabad for the financial support received for the nanoindenter used in this study.

## References

- Alkorta J, Martinez-Esnaola JM, Sevillano JG (2008) Critical examination of strain-rate sensitivity measurement by nanoindentation methods: application to severely deformed niobium. *Acta Mater* 56:884–893. <https://doi.org/10.1016/j.actamat.2007.10.039>
- Armstrong DEJ, Hardie CD, Gibson JSKL, Bushby AJ, Edmondson PD, Roberts SG (2015) Small-scale characterisation of irradiated nuclear materials: part II nanoindentation and micro-cantilever testing of ion irradiated nuclear materials. *J Nucl Mater* 462:374–381. <https://doi.org/10.1016/j.jnucmat.2015.01.053>
- Bagherifard S, Ghelichi R, Mario G (2012) On the shot peening surface coverage and its assessment by means of finite element simulation: a critical review and some original developments. *Appl Surf Sci* 259:186–194. <https://doi.org/10.1016/j.apsusc.2012.07.017>
- Chinh NQ, Szommer P (2014) Mathematical description of indentation creep and its application for the determination of strain rate sensitivity. *Mater Sci Eng A* 611:333–336. <https://doi.org/10.1016/j.msea.2014.06.011>
- Dayal P et al (2013) Effect of double ion implantation and irradiation by Ar and He ions on nano-indentation hardness of metallic alloys. *J Nucl Mater* 438:108–115. <https://doi.org/10.1016/j.jnucmat.2013.02.078>
- Grievson EM, Armstrong DEJ, Xu S, Roberts SG (2012) Compression of self-ion implanted iron micropillars. *J Nucl Mater* 430:119–124. <https://doi.org/10.1016/j.jnucmat.2012.06.014>

- Hardie CD, Roberts SG, Bushby AJ (2015) Understanding the effects of ion irradiation using nanoindentation techniques. *J Nucl Mater* 462:391–401. <https://doi.org/10.1016/j.jnucmat.2014.11.066>
- Hattar K, Buchheit T, Kotula P, McGinnis A, Brewer L (2012) Nanoindentation and TEM characterization of ion irradiated 316L stainless steels Energy Technology. In: Carbon dioxide management and other technologies Chapter 43. Wiley, USA
- Hosemann P, Swadener JG, Kiener D, Was GS, Maloy SA, Li N (2008) An exploratory study to determine applicability of nano-hardness and micro-compression measurements for yield stress estimation. *J Nucl Mater* 375:135–143. <https://doi.org/10.1016/j.jnucmat.2007.11.004>
- Hosemann P, Vieh C, Greco RR, Kabra S, Valdez JA, Cappiello MJ, Maloy SA (2009) Nanoindentation on ion irradiated steels. *J Nucl Mater* 389:239–247. <https://doi.org/10.1016/j.jnucmat.2009.02.026>
- Hosemann P, Kiener D, Wang Y, Maloy SA (2012) Issues to consider using nano indentation on shallow ion beam irradiated materials. *J Nucl Mater* 425:136–139. <https://doi.org/10.1016/j.jnucmat.2011.11.070>
- Kalainathan S, Prabhakaran S (2016) Recent development and future perspectives of low energy laser shock peening. *Opt Laser Technol* 81:137–144. <https://doi.org/10.1016/j.optlastec.2016.02.007>
- Kasada R, Konishi S, Hamaguchi D, Ando M, Tanigawa H (2016) Evaluation of strain-rate sensitivity of ion-irradiated austenitic steel using strain-rate jump nanoindentation tests. *Fusion Eng Des* 109–111:1507–1510. <https://doi.org/10.1016/j.fusengdes.2015.11.041>
- Ma G, Ling X (2011) Study on hardness and elastic modulus of surface nanostructured 304 stainless steel using two mechanical methods. *J Press Vessel Technol* 133:034501. <https://doi.org/10.1115/1.4002554>
- Maier-Kiener V, Durst K (2017) Advanced nanoindentation testing for studying strain-rate sensitivity and activation volume. *JOM* 69:2246–2255. <https://doi.org/10.1007/s11837-017-2536-y>
- Mannan SL, Chetal SC, Raj B, Bhoje SB (2003) Selection of materials for prototype fast breeder reactor proceedings of the seminar held on materials R&D for PFBR, IGCAR, Kalpakkam pp 9–44
- Montross CS, Brandt M, Swain MV (2001) Self-limiting hardness changes in laser peened 6061-t6 aluminium. *Surf Eng* 17:477–482
- Montross CS, Wei T, Ye L, Clark G, Mai Y-W (2002) Laser shock processing and its effects on microstructure and properties of metal alloys: a review. *Int J Fatigue* 24:1021–1036
- Mordyuk BN, Milman YV, Iefimov MO, Prokopenko GI, Silberschmidt VV, Danylenko MI, Kotko AV (2008) Characterization of ultrasonically peened and laser-shock peened surface layers of AISI 321 stainless steel. *Surf Coat Technol* 202:4875–4883
- Nakano H, Tsuyama M, Miyauti S, Shibayanagi T, Tsukamoto M, Abe N (2010) Femtosecond and nanosecond laser peening of stainless steel. *J Laser Micro/Nanoeng* 5:175–178
- Oliver WC, Pharr GM (1992) An improved technique for determining hardness and elastic modulus using load and displacement sensing indentation experiments. *J Mater Res* 7:1564–1583
- Oliver WC, Pharr GM (2004) Measurement of hardness and elastic modulus by instrumented indentation: advances in understanding and refinements to methodology. *J Mater Res* 19:3–20
- Reichardt A, Ionescu M, Davis J, Edwards L, Harrison RP, Hosemann P, Bhattacharyya D (2015) In situ micro tensile testing of He +2 ion irradiated and implanted single crystal nickel film. *Acta Mater* 100:147–154. <https://doi.org/10.1016/j.actamat.2015.08.028>
- Saleh M et al (2016) Relationship between damage and hardness profiles in ion irradiated SS316 using nanoindentation—experiments and modelling. *Int J Plast* 86:151–169. <https://doi.org/10.1016/j.ijplas.2016.08.006>
- Sharma G, Sarkar A, Varshney J, Ramamurthy U, Kumar A, Gupta SK, Chakravarty JK (2011) Effect of irradiation on the microstructure and mechanical behavior of nanocrystalline nickel. *Scripta Mater* 65:727–730. <https://doi.org/10.1016/j.scriptamat.2011.07.021>
- Sharon JA, Hattar K, Boyce BL, Brewer LN (2013) Compressive properties of (110) Cu micro-pillars after high-dose self-ion irradiation. *Mate Res Lett* 2:57–62. <https://doi.org/10.1080/21663831.2013.859179>
- Sudharshan Phani P, Oliver WC, Pharr GM (2017) On the measurement of power law creep parameters from instrumented indentation. *JOM* 69:2229–2236. <https://doi.org/10.1007/s11837-017-2535-z>
- Suri AK, Krishnamurthy N, Batra IS (2010) Materials issues in fusion reactors. *J Phys Conf Ser* 208:012001. <https://doi.org/10.1088/1742-6596/208/1/012001>
- Varam S, Narayana PVSL, Prasad MD, Chakravarty D, Rajulapati KV, Bhanu Sankara Rao K (2014a) Strain rate sensitivity of bulk multi-phase nanocrystalline Al–W-based alloy. *Philos Mag Lett* 94:582–591. <https://doi.org/10.1080/09500839.2014.948522>
- Varam S, Rajulapati KV, Bhanu Sankara Rao K, Scattergood RO, Murty KL, Koch CC (2014b) Loading rate-dependent mechanical properties of bulk two-phase nanocrystalline Al–Pb alloys studied by nanoindentation. *Metall Mater Trans A* 45:5249–5258. <https://doi.org/10.1007/s11661-014-2425-8>
- Varam S, Prasad MD, Rao KBS, Rajulapati KV (2016) Mechanical properties of in situ consolidated nanocrystalline multi-phase Al–Pb–W alloy studied by nanoindentation. *Philos Mag* 96:3671–3685. <https://doi.org/10.1080/14786435.2016.1234721>
- Yella P, Venkateswarlu P, Buddu RK, Ravi N, Rao KBS, Kiran PP, Rajulapati KV (2018a) Role of sacrificial layers on surface characteristics of laser shock peened SS304 plates. *Opt Laser Technol* 107:142–149
- Yella P, Venkateswarlu P, Buddu RK, Vidyasagar DV, Sankara Rao KB, Kiran PP, Rajulapati KV (2018b) Laser shock peening studies on SS316LN plate with various sacrificial layers. *Appl Surf Sci* 435:271–280. <https://doi.org/10.1016/j.apsusc.2017.11.088>
- Yella P, Rajulapati KV, Prasad Reddy GV, Sandhya R, Prem Kiran P, Buddu RK, Bhanu Sankara Rao K (2019) Effect of laser shock peening on high cycle fatigue characteristics of 316LN stainless steel. *Int J Press Vessels Pip* 176:103972. <https://doi.org/10.1016/j.ijpvp.2019.103972>

**Publisher's Note** Springer Nature remains neutral with regard to jurisdictional claims in published maps and institutional affiliations.